NASA TN D-1104

TECHNICAL NOTE

D-1104

EXPERIMENTAL STUDY OF COMBINED FORCED AND FREE LAMINAR CONVECTION IN A VERTICAL TUBE

By Theodore M. Hallman

Lewis Research Center
Cleveland, Ohio

NATIONAL AERONAUTICS AND SPACE ADMINISTRATION

WASHINGTON

December 1961

NATIONAL AERONAUTICS AND SPACE ADMINISTRATION

TECHNICAL NOTE D-1104

EXPERIMENTAL STUDY OF COMBINED FORCED AND FREE LAMINAR CONVECTION IN A VERTICAL TUBE[1]

By Theodore M. Hallman

SUMMARY

An apparatus was built to verify an analysis of combined forced and free convection in a vertical tube with uniform wall heat flux and to determine the limits of the analysis. The test section was electrically heated by resistance heating of the tube wall and was instrumented with thermocouples in such a way that detailed thermal entrance heat-transfer coefficients could be obtained for both upflow and downflow and any asymmetry in wall temperature could be detected.

The experiments showed that fully developed heat-transfer results, predicted by a previous analysis, were confirmed over the range of Rayleigh numbers investigated. The concept of "locally fully developed" heat transfer was established. This concept involves the assumption that the fully developed heat-transfer analysis can be applied locally even though the Rayleigh number is varying along the tube because of physical-property variations with temperature.

Thermal entrance region data were obtained for pure forced convection and for combined forced and free convection. The analysis of laminar pure forced convection in the thermal entrance region conducted by Siegel, Sparrow, and Hallman was experimentally confirmed. A transition to an eddy motion, indicated by a fluctuation in wall temperature, was found in many of the upflow runs. A stability correlation was found.

The fully developed Nusselt numbers in downflow were below those for pure forced convection but fell about 10 percent above the analytical curve. Quite large circumferential variations in wall temperature were observed in downflow as compared with those encountered in upflow, and the fully developed Nusselt numbers reported are based on average wall temperatures determined by averaging the readings of two diametrically opposite wall thermocouples at each axial position. With larger heating rates in downflow the wall temperature distributions strongly suggested a cell flow near the bottom. At still larger heating rates the wall temperatures varied in a periodic way.

---

[1]The information presented herein is an abbreviated form of a thesis entitled "Combined Forced and Free Convection in a Vertical Tube" submitted in partial fulfillment of the requirements for the degree of Doctor of Philosophy at Purdue University, 1958.

INTRODUCTION

Description of the Problem

A description of the problem considered in this report is perhaps best introduced by considering the simple physical system illustrated in figure 1(a). This sketch illustrates a round tube of finite length immersed in a large body of fluid which is at some uniform temperature. The tube is positioned with its axis vertical, and the outer surface of the tube is perfectly insulated.

If there is no heat transfer to or work done on the system, the fluid remains at rest, the buoyant forces on each element of fluid being exactly balanced by the hydrostatic pressure. However, if the tube is heated in some way, the fluid within the tube changes temperature and its density decreases.[2] This reduced density causes an increase in the buoyant force, and the fluid tends to rise and pass out the top of the tube, where it mixes with the large mass of unheated surrounding fluid. This action draws cold fluid into the bottom of the tube, and hence a pumping action occurs. This type of flow and heat transfer is commonly called free convection.

If the surrounding fluid is replaced by the cooler piping system and pump shown in figure 1(b) and the cooling and pumping rates are controlled to maintain the temperatures t_a and t_e unchanged, conditions are unchanged inside the pipe. This situation is commonly called combined forced and free convection.

There is one important distinction between the two situations just described. In the first situation, for a given heating rate in the tube, there is a unique flow rate established, which is such that the pressure drop through the tube is exactly balanced by the net buoyant force. In the second situation, on the other hand, there is freedom to adjust the pump flow rate to any desired value. Of course, when the flow rate is changed, the heat-transfer rate must be changed in order to keep t_a and t_e unchanged. The buoyant forces still exist, regardless of the flow rate, but only one flow rate corresponds to the free-convection situation. There is no basic difference in the case of "pure free convection"; it is merely a special case of the so-called combined forced and free convection.

When the flow rate is gradually increased in the apparatus shown in figure 1(b), the buoyant force becomes less and less important in comparison with the pumping force. The term "forced convection" is used to describe the limiting situation when the buoyant forces are negligible. Since all fluids change in density when heated, pure forced convection

---

[2]Most fluids behave in this manner, although there are exceptions.

is never exactly realized. One of the goals of the present study was to establish when the buoyant, or free-convection effect, is negligible.

There are a great many possible variations to the problem considered. The tube walls may be heated in different ways (two common ways are uniform wall temperature and uniform wall heat flux). In addition, internal heat sources, due to chemical or nuclear reactions, either uniform or nonuniform, may be present within the fluid inside the tube. The tube diameter and length may be varied, as well as the kind of fluid. Finally, the cross-sectional shape may be round, square, or some other shape.

When the cool fluid enters the bottom of the tube, it is heated and rises. If the tube is long enough, and if the boundary conditions are suitable, the radial velocity and temperature profiles beyond a certain inlet length are similar to the corresponding profiles at other cross sections farther up the tube. This region is known as the region of "fully developed" flow and heat transfer. The length of the tube required to establish similar profiles is called the "entrance length."

The problem considered herein is one of combined forced and free laminar convection in a vertical round tube. The boundary conditions considered are uniform wall heat flux. No heating was present within the fluid.

The transfer of heat by combined forced and free convection in vertical channels (more generally, in channels in which the flow is parallel to the direction of the body force, i.e., gravity or centrifugal) is very common, but only in recent years has much attention been placed on determining the characteristics of such systems. Possible uses in nuclear reactor or turbine blade cooling are mainly responsible for recent interest in this mode of heat transfer.

Purpose of Experiment

The purpose of the experiment was to check the analysis of reference 1 and also to provide information about the region of applicability, that is, the transition Reynolds and Rayleigh numbers and the entrance lengths required for the flow to become fully developed. The limiting case of pure laminar forced convection, including thermal entrance effects, was also to be studied.

The specific case chosen for the experiment was combined forced and free laminar convection in a vertical round tube with uniform wall heat flux and no internal heat generation. Provision was made for both upflow with heating and downflow with heating, that is, both positive and negative Rayleigh numbers. The apparatus was designed to be suitable

as well for obtaining data on pure forced convection, both laminar and turbulent. Previous data (refs. 2 and 3) for the laminar region were subject to large experimental error.

SURVEY OF THE LITERATURE

Theoretical Investigations

The analysis of the case of combined forced and free convection in a vertical round tube with uniform wall heat flux is considered in references 1 and 4 to 8. None of these analyses consider entrance effects or turbulence or transition to turbulence. The limiting case of pure forced convection in thermal entrance regions is analyzed in reference 9.

Experimental Investigations

Some data on combined forced and free convection in vertical pipes with uniform wall heat flux are given in references 2, 3, 10, and 11. Reference 11 includes some information on transition to turbulence. Since wall temperatures were not measured it was not possible to calculate Nusselt numbers.

Comparison of Previous Experiments with Analysis

The experimental data from other experiments are compared with the analysis of reference 1 in figure 2. The solid line represents the analysis. The Nusselt numbers in the range $100 \leq Ra \leq 10{,}000$ are accurately approximated by the equation

$$Nu = 1.40\ Ra^{0.23} \tag{1}$$

This relation is shown in figure 2 by the dashed line. (Symbols are defined in appendix A.)

The experimental points shown as squares in figure 2 are the data of reference 10 for high-pressure water (2000 and 1500 lb/sq in. abs) flowing upward in a vertical electrically heated tube. The tube had an inside diameter of 0.1305 inch and a length of 9 inches and thus an L/D of 80.

These data fall below the analysis. In reference 12 these same data are compared on a different basis with other experimental data and are found to fall low there as well.

Two other experiments have provided data for lower Rayleigh numbers. These experiments were designed for pure forced convective flow, but the Rayleigh numbers were high enough in some cases to show significant free convective effects. The first experiment is that of Gross (ref. 2). These data are shown as circles in figure 2 and are for water in upflow in an electrically heated tube. Three tubes of 0.2244-, 0.305-, and 0.432-inch inside diameter were used.

Heated tube lengths varied from 2 to 5 feet. Local heat-transfer data were reported but only data which satisfy the condition

$$\frac{2x/D}{RePr} > 0.085$$

are plotted here.[3] This is the condition found necessary in reference 9 for the Nusselt numbers for pure forced convection laminar heat transfer to be within 5 percent of the fully developed value. This condition is for a fully developed entering velocity profile and a uniform wall heat flux corresponding to this experiment. Also, all data for Reynolds numbers greater than 2000 were not plotted. It is seen that the scatter in the data of reference 2 is quite large. The higher values of Nusselt numbers at low and high Rayleigh numbers are believed to be caused by bus bar conduction lowering the tube wall temperatures at entrance and exit. Despite the large scatter, the trend in the data away from the pure forced convection Nusselt number of 4.36 is largely accounted for by the analytical curve shown.

Two data points at low Rayleigh number from an experiment reported in reference 3 are shown as triangles in figure 2. These data are for water flowing upward in an electrically heated vertical tube. The tube had an inside diameter of 0.2244 inch and a heated length of 12 feet. The entering velocity profile was probably nearly uniform, so the only data shown are those for which

$$\frac{2x/D}{RePr} > 0.191$$

This is the requirement for the Nusselt numbers to be within 5 percent of the fully developed value if the entering velocity profile is uniform and the wall heat flux is uniform (ref. 13).

---

[3]For this reason fewer points are shown in figure 2 than are shown in figure 7 of reference 1.

DESCRIPTION OF APPARATUS

Flow Loop

A schematic diagram of the heat-transfer loop is shown in figure 3. Distilled and deionized water was circulated as the heat-transfer medium. A constant-head tank was used to ensure a steady flow through the test section. This was found to be necessary from preliminary tests. The water was de-aerated by being heated to the boiling point in the head tank, and it was then cooled to the desired temperature by water cooling coils directly beneath the head tank. The flow was down a 44-foot insulated standpipe to an insulation tank which contained the heated test section. The test section was surrounded by seven concentric aluminum-foil radiation guards. The tank air pressure was maintained at about 1 micron of mercury. Such an arrangement gave a rapid time response and nearly negligible heat losses.

In upflow the fluid passed first through a bottom mixing box, where the inlet bulk temperature was measured, and then up through a 3-foot insulated hydrodynamic approach section of 5/16-inch bore. This section had a length-to-diameter ratio of 115 to allow the velocity profile to become fully developed. The water then flowed without interruption through a Teflon insulating disk and into the heated test section. The Inconel test section also had a 5/16-inch bore and was 3 feet long ($L/D = 115$). It was heated by passing low-voltage alternating current axially through the tube wall. Thermocouples attached to the outer wall allowed a determination of local wall temperature.

The heated water passed out through a second Teflon insulating disk and then to an outlet mixing box, where the outlet bulk temperature was measured. The water left the insulation tank at the top and was cooled to room temperature in a heat exchanger. It was then filtered and passed through a flow control needle valve.

The discharge from the flow control needle valve went into two glass burettes, where the flow rate was determined. This measurement was accomplished by determining the time required to fill the burettes when the outlet valve was closed. The time was measured automatically by a combination of electronic relays and an electronic timer. Figure 3 illustrates this system. A rotameter was also used to give a rough indication of the flow rate.

The water leaving the burette went to a sump tank and then was pumped back up to an overflow tank by a sump pump. A second circulating pump transferred the water from the overflow tank through a heated pipe to the head tank. The purpose of the heater was to heat the water to near the boiling point and thus de-aerate it. The overflow from the head tank returned to the overflow tank through a cooler. The

temperature of the water in the head tank was held near the boiling point by a thermoswitch-heater combination.

A bypass mixed-bed ion exchanger not shown in figure 3 was connected between the bottom of the standpipe and the sump tank. A constant flow through the ion exchanger maintained the high purity of the distilled water.

Details of the various components of the flow loop are given in reference 3.

For downflow the water entered the insulation tank at the top and left at the bottom. The rest of the flow loop was unchanged. The starting length for downflow was considerably shorter, being about 13 diameters.

Several modifications were made to the apparatus after 17 runs had been made. One change was the addition of a temperature regulating bath to control water inlet temperature. This bath reduced inlet temperature fluctuations from 1° F to less than 0.2° F. Another modification was the installation of an immersion heater in the head tank to replace a wrap-around heater on the inlet line. This change allowed more reliable operation and a steadier head tank temperature. A third modification was an improvement in the vibration isolation of the insulation tank. Vibrations from the vacuum pump had been felt in the insulation tank and there was a possibility that this could cause an early transition to turbulent flow.

Test Section and Approach Section

The test section was a resistance-heated Inconel tube with a 0.3130-inch bore and a 0.0312-inch wall thickness. The length was 36.030 inches, and the length-to-diameter ratio was therefore about 115. A sketch of the test section and approach section is shown in figure 4, and a photograph of the assembly is given in figure 5. The approach section in downflow had a length-to-diameter ratio of 13.

Fifty-eight iron-constantan thermocouples were spot-welded to the outside of the test section in 29 diametrically opposed pairs. A detail of the method of attachment is shown in figure 4. A listing of their exact locations is given in reference 5. The axial spacing of the thermocouples near each end was small in order to allow an accurate determination of entrance region wall temperatures for both upflow and downflow. Axially adjacent pairs of thermocouples were positioned 90° apart. This was done to facilitate detection of any asymmetry in wall temperature distribution.

Circular copper flanges were silver soldered to each end of the test section. The power leads were connected to the outer circumference of these flanges. Potential leads were soldered to each flange. These flanges also contained thermocouples which were used to determine heat losses as is described in reference 5. The test section was connected to and insulated from the approach and exit sections by Teflon disk spacers.

A detail drawing of the approach section is given in figure 4. The approach section was identical to the test section except that it was not heated and had fewer thermocouples attached to it. The approach section, Teflon spacers, test section, and exit section were all very carefully alined, doweled, and bolted in order to ensure that the flow pattern would not be disturbed when the water passed from one section to another.

Test-Section Insulation

The small heat-transfer coefficients encountered in laminar flow require an insulation superior to glass or quartz wool. Two possibilities which seemed promising were a vacuum bottle or a powdered insulation under vacuum. The first approach was followed, because it was felt that the large time constants involved with a low-thermal-diffusivity material would make operation difficult.

Seven concentric cylinders of aluminum foil were mounted between the test section and the insulation tank to act as radiation shields.

The radial heat loss was measured with the test section drained and plugged. A plot of heat loss per foot is shown in figure 6. The loss is nearly a linear function of temperature difference. It is possible to compute a "thermal conductivity" of the insulation tank. It is about 0.0046 Btu/(hr)(ft)(^{o}F) compared with 0.023 Btu/(hr)(ft)(^{o}F) for glass wool. Thus it is about five times as effective. The measurements were all made at the tank operating pressure of 0.6 to 1 micron of mercury. This radial heat loss is nearly negligible for most runs but was included in all calculations.

Power Supply

The test section was resistance heated by the power supply shown schematically in figure 7. Power was supplied from a 230-volt supply, and the current passed through a 5-kilovolt-ampere electronic voltage regulator with a line voltage regulation accuracy of ±0.1 percent. The output then passed to a variable autotransformer and then through two 2-kilovolt-ampere stepdown transformers in parallel, which reduced the

voltage to a maximum of 11 volts. From the transformers the current flowed directly to the power lead connections on top of the insulation tank.

Power Measuring Instruments

Power was measured by a multiplied-deflection a-c potentiometer similar to the one described in reference 14. This method has the advantage that the accuracy is limited only by the full-scale accuracy of the meters and is independent of power level. This was highly desirable because power ranged from 0.17 watt on the heat loss measurements to 4000 watts on the higher power heat-transfer runs. An a-c potentiometer was of value also, because the low voltage drops across the test section made it difficult to use a wattmeter directly. The voltmeter and ammeter were calibrated in an NASA instruments laboratory and correction charts were used with them. The wattmeter was calibrated with a resistor whose d-c resistance was accurately measured on a Kelvin bridge. The wattmeter readings were compared with I^2R of the test section, and they always agreed to within 2 percent. The power factor was very nearly unity at all times.

Temperature Measuring System

Iron-constantan thermocouples were used throughout for temperature measurement. Test-section and mixing-box thermocouples were carefully calibrated. Details of the calibration procedure are given in reference 5. The tables of NBS circular 561 were used for uncalibrated thermocouples.

A circuit diagram for the thermocouples is shown in figure 8. Test-section wall thermocouples and the outlet mixing-box thermocouple were always read with respect to the inlet mixing-box thermocouple. Since both upflow and downflow runs were made, provision was made for a reversing switch to interchange roles of the mixing boxes. Each mixing-box junction could be read with respect to an ice junction in order to establish the absolute temperature level of the system. A self-balancing potentiometer was used to obtain rough readings when the system was approaching steady state.

A Rubicon potentiometer, Model B, was used to measure thermocouple voltages. An electronic null indicator, with a voltage sensitivity of 1 microvolt per small division, served in place of a conventional light beam galvanometer to indicate the matching of potentiometer and thermocouple voltages.

All thermocouple wires passed to a junction box. The thermocouple wires on the test section and in the mixing boxes were 36 gage and were all cut from the same spools of wire. At the junction box the wires were increased in size to make the leads more durable. Iron-constantan wire was used throughout the thermocouple circuits. From the junction box the leads went to a switch box, which housed all switches. Leads from the switch box passed to the self-balancing potentiometer and the Rubicon potentiometer.

The junction box and switch box were of identical construction. All thermocouple junctions were contained in a copper box. This copper box was surrounded by several inches of foamed-plastic insulation, which in turn was contained in a wooden box. The purpose of this type of construction was to produce a uniform temperature at the junction of each pair of thermocouple wires. Even though the box temperature might change because of changes in ambient conditions, both thermocouple junctions would change in the same way and thus prevent any stray voltages from being developed.

EXPERIMENTAL PROCEDURE

The experimental data were taken in the following manner. Several runs at different heating rates were usually taken at one flow rate. When a new flow rate was set by adjusting the flow control needle valve, it was generally necessary to allow the apparatus to run overnight in order that steady conditions would be established. When the flow was steady and the inlet water temperature variations were tolerable, the power was turned on and set at the desired value. Usually a half hour was sufficient to attain equilibrium. This time was adequate because of the fast time response of the thin aluminum radiation guards.

Readings were taken of volts, amperes, watts, voltage divider ratio, current transformer ratio, water inlet temperature above ice point, water outlet temperature above ice point, and bulk temperature rise before, half way through, and after the reading of wall temperature thermocouples. As many readings of the time to fill burettes were taken as was possible during the run. Besides wall temperature readings, data were taken on room temperature, flange temperatures, and approach section temperatures.

At the completion of a run the power level was readjusted to obtain a different Rayleigh number.

EXPERIMENTAL RESULTS

The important results of the experiment are presented and discussed in this section, and a discussion of accuracy and anomalies of the

experiment is given in appendix B. The experimental results are tabulated in reference 5.

Results for Heating with Upflow

Fully developed heat transfer. - The primary objective of this experiment was to verify the analysis which was made for the condition of fully developed heat transfer and constant fluid properties. The data which are believed to be fully developed and which were steady (nonfluctuating) are shown in figure 9. The solid line is the predicted curve of the analysis, which is shown in figure 2 also. It is apparent that these data confirm the analysis over the range presented. The data at high values of Rayleigh number show some scatter and also seem to be slightly below the analytical curve. Physical properties were evaluated at the film temperature; some of the scatter may be due to physical property variations with temperature. However, it is believed that these data are low at high Rayleigh numbers because of a peculiar entrance effect. This is discussed later when the thermal entrance region results are presented.

Another observation to be made from figure 9 is that it is very difficult to confirm the pure forced convection fully developed Nusselt number of 48/11 (4.36) experimentally because of the influence of free convection effects. The lowest Rayleigh number attainable with reasonable accuracy was about 25. This gives a Nusselt number of 4.62, about 6 percent above the zero Rayleigh number value.

Thermal entrance region data. - Having confirmed the fully developed analysis, a question arises as to what length is required to produce the fully developed condition. An investigation of this thermal entrance length may be made by means of the experiment.

The pure forced convection (zero Rayleigh number) analysis of reference 9 provides a basis for comparison of thermal entrance region data. The Nusselt numbers very near the heated entrance will be independent of the heating rate, because the Nusselt number is determined only by the flow pattern. The velocity profile will not be distorted from its entering parabolic shape until a temperature pattern is created in the fluid. This temperature pattern then creates radial density differences, which, in turn, distort the parabolic velocity profile and thus change the Nusselt numbers from the pure forced convection values. A certain heated length is required for this profile to be distorted.

The pure forced convection analysis results in a single relation between Nusselt number and the parameter $\frac{2x/D}{RePr}$. It is reasonable, then, to present the data in terms of these variables, with Rayleigh number as

a parameter. Such a comparison is given in figure 10. The solid curve is the zero Rayleigh number analysis (ref. 9), and the data shown are for a very low Rayleigh number run and for a typical high Rayleigh number run. Numbers beside the data indicate local Rayleigh numbers.

The very low Rayleigh number run agrees well with the pure forced convection analysis of reference 9. These data are typical of all low Rayleigh number runs.

The high Rayleigh number run agrees with the zero Rayleigh number analysis very near the entrance, but soon breaks away, goes through a minimum, and rises again. The dashed line is the fully developed combined forced and free convection analysis (ref. 1) applied locally. The Rayleigh number increases toward the pipe exit because of physical property variations. The agreement between the data and the dashed line indicates that the concept of a "locally fully developed" heat transfer is a valid one. Again, this run is typical of many such runs taken and tabulated in tables II and III of reference 5.

The highest Rayleigh number run in which entrance data were obtained is shown on the same type of plot in figure 11. Again the analysis (ref. 1) applied locally is shown as a dashed line. In this run the data fall below the analysis and then gradually climb to approach the analytical curve. The effect is most pronounced in this highest Rayleigh number run. This effect was observed to a lesser extent, in lower Rayleigh number runs as well. It may be due to experimental error, but this is considered unlikely. At high values of Rayleigh number an "undershoot" occurs, because the large velocity profile distortion involved requires a considerable length in which to develop.

This argument and discussion are based on somewhat meager data, but they are believed to explain the low Nusselt numbers observed at high Rayleigh numbers in figure 9. These particular data were taken in the vicinity of the transition points, discussed later, and complete entrance data were not obtained. It is likely that some of these data are in the "undershoot" region and hence would fall below the analysis.

For pure forced convection, it is shown in reference 9 that the value of $(2x/D)/RePr$ at which the Nusselt number came to within 5 percent of its fully developed value was 0.085.

The entrance length for the high Rayleigh number run (run (U14)) shown in figure 10 was taken to be

$$\left(\frac{2x/D}{RePr}\right)_{fd} = 0.034$$

and for run (U24)(fig. 11) this value was taken to be about 0.075 where the data become asymptotic to the analysis, applied locally. Values of $(2x/D)/RePr$ at which the data became parallel to the analytical curve are plotted in figure 12. The scatter in the data is very large because of the difficulty in accurately estimating when the fully developed condition is reached. However, the trend definitely indicates a decrease in thermal entrance length with increase in Rayleigh number followed by an increase at large Rayleigh numbers.

Transition data. - A transition from steady laminar flow to a slow, apparently random, eddy flow was observed on some runs. This was evidenced by wall temperature fluctuations appearing on the upper portions of the heated tube. Temperature records taken with a photoelectric recorder are shown in figure 13 for a typical run in which transition occurred. With an increase in heating rate, at a constant flow rate, the transition point would travel down the tube toward the entrance. If the flow rate were increased, keeping the Rayleigh number constant, the transition point would travel up and eventually out the tube exit.

Special runs were made in order to gather data on this transition. A tentative correlation of these transition data is shown in figure 14. Plotted here against $\frac{RePr}{2x/D}$ is a special Rayleigh number defined by

$$Ra_D = \frac{\rho^2 \beta g (t_w - t_m) D^3}{\mu^2} Pr \tag{2}$$

Physical properties are evaluated at the film temperature. The dashed line is given by the equation

$$Ra_D = 9470 \left(\frac{RePr}{2x/D} \right)^{1.83} \tag{3}$$

Since thermocouples were located only at 2-inch intervals in most cases, it was difficult to locate the transition x/D exactly. In addition, the transition point was difficult to locate precisely, because the wall temperature fluctuations were damped by the heat capacity of the tube wall. The correlation is probably adequate for most applications, however.

Since transition is likely to be affected by such things as vibration level, tube nonuniformities, the tube being not exactly vertical, and so forth, it is recommended that additional data be obtained in another apparatus.

Transition data recently obtained are reported in reference 11. The transition point was detected by injecting dye into the water upstream

and observing when the dye stream began to fluctuate at the exit of a transparent tube. These data are shown in figure 14. Since observations were made at the exit only, no x/D variation could be made. The transition point for stream fluctuation occurs at lower values of Ra_D than for wall temperature fluctuations. This would be expected, since the stream fluctuations would have to build up to some magnitude in order to transport heat radially from the wall.

Selection of data. - A discussion of the selection of upflow data is perhaps best introduced by referring to two representative plots of temperature against x/D.

Figure 15(a) shows a representative wall temperature plot for a low Peclet number (RePr) run. Generally there were two thermocouples at each x/D, located diametrically opposite. In some cases, however, only one thermocouple was operative. The dashed line shown is a curve drawn through the points obtained by averaging temperatures only at axial locations where both thermocouples were operative. The circles represent individual thermocouple temperatures. Several observations can be made from this figure. First, a very smooth curve can be drawn through the averaged data. Second, an asymmetric wall temperature distribution is apparent near the tube exit. Third, a slight rise in temperature exists in the first several diameters.

The fact that a smooth curve can be drawn through the averaged data was used to reject data points obtained when only one thermocouple existed at a location, since these points generally did not fall on the smooth curve because of the asymmetry in wall temperature. The asymmetry in wall temperature was more severe at higher powers. This could be caused by a nonuniform tube wall causing nonuniform heating, or it could be caused by an asymmetric flow pattern set up by free convection effects. It is believed to be principally the latter, because in downflow the asymmetry, which had been near the top in upflow, now appeared near the bottom. This is discussed in the next section. The theory predicts that the wall temperatures should approach the fluid bulk temperature at the entrance. This does not happen in the experiment; in fact, there is a slight temperature rise very near the entrance. This is caused by joulean heat from the bottom bus bar being conducted into the bottom flange. The first few temperatures were inaccurate because of this.

Figure 15(b) shows a representative wall temperature plot for a high Peclet number run. The small rise in temperature near the entrance is still present. The asymmetry in wall temperature is now more severe at the higher power. The striking thing about this plot, however, is the dip in wall temperature near the exit of the tube. This dip was present in all runs with Peclet numbers of 1500 or more. The dips had a minimum at a constant x/D of about 95 (about 6 in. from exit) which did not seem to shift under any circumstances. The explanation for this dip is

unknown. It has been established that it is not (1) due to heat conduction through a bundle of thermocouple leads which leaves at this point, (2) due to a heat leak in the insulation at this point, (3) caused by a nonuniform tube in this region, or (4) a false temperature caused by a-c effects on the thermocouple circuits. No dip occurred in any downflow runs. Data in this region are not presented in the results (although they are tabulated in ref. 5) because the reason for this behavior is not known.

Results for Heating with Downflow

The downflow runs were characterized by an asymmetry in wall temperature which became more severe as the heating rate was increased. For the highest heating rates, the flow became unsteady, and the wall temperatures in the lower portion of the heated tube oscillated in a periodic way.

Fully developed heat transfer. - The data which appeared to be fully developed are presented in figure 16 as a plot of Nusselt number against Rayleigh number. The line with which the data are to be compared is the solid line labeled negative Rayleigh number. This line is derived in reference 5. The two dashed lines, for zero Rayleigh number and for positive Rayleigh number, are included to provide a comparison with previously discussed upflow results.

It is seen that most of the data fall about 10 percent above the predicted curve. Each point shown is based on a wall temperature obtained by averaging the temperatures of two thermocouples placed diametrically opposite. These temperature differences were as high as 7° F in some cases when the axial temperature rise over the length of the tube was only 23° F. It is believed that this asymmetry in wall temperature is caused by an asymmetry in flow pattern. It is not surprising, therefore, that the data do not agree exactly with the analysis.

Even though most of the data fall above the analysis, the trend in the data is correctly predicted. All the Nusselt numbers are below the pure forced convection value of 4.36, and considerably below the data which have exactly the same heating and flow conditions but which have the direction of flow reversed.

Thermal entrance region data. - A typical plot of Nusselt number against the parameter $(2x/D)/RePr$ is shown in figure 17. The data do not reach the fully developed analysis (dashed line) for reasons already discussed. The entrance lengths appear to be longer than for pure forced convection, although it is difficult to estimate entrance lengths accurately. Estimation is difficult mainly because the local Rayleigh number decreases (negatively) with length and so the "local fully developed"

Nusselt numbers decrease with length. The range of Rayleigh numbers was quite small. A rough estimate for entrance length is

$$\left(\frac{2x/D}{RePr}\right)_{fd} = 0.1$$

if the Rayleigh number is not below -120.

Closer to the entrance, the Nusselt numbers agree quite well with the pure forced convection analysis (as they did for positive Rayleigh numbers). The two low points, nearest the entrance, are believed to be caused by bus bar conduction errors.

The approach section length-to-diameter ratio for downflow was about 13. The length-to-diameter ratio required for fully developed flow is about 0.05 Re (ref. 15). Most of the runs were made with fully developed flow at the entrance to the heated section. The highest Reynolds number used was 330, which would require an L/D of 19 for fully developed flow.

Axially asymmetric and periodic flow. - The wall temperature was found to vary around the circumference of the tube for all downflow runs. For a given run, the variations became worse from inlet to outlet (top to bottom), and for different runs, the variations became more severe with increasing heating rates. For low power runs, the averaging of diametrically opposite thermocouple readings gave a smooth curve from top to bottom (fig. 18(a)), whereas for higher power runs an apparent discontinuity in this "average" wall temperature curve is indicated (fig. 18(b)). The variation across the tube below this discontinuity became very large in some cases, being as high as 20° F. One might speculate that above this discontinuity the flow is always down, but is asymmetric; below the discontinuity a cell flow may be set up, with a large crossflow at the position of the discontinuity. Since it was not possible to observe the flow, however, one can only speculate.

With a still greater increase in heating rate, the wall temperatures became unsteady in the lower portions of the tube. The variations were nearly periodic in nature. The amplitude of the variations was different at different points on the tube, but the frequency was the same everywhere. Figure 19 gives a record of the fluctuations observed for one particular run.[4] The variations were more regular in the upper part of the region than in the lower part. The frequency was about 0.8 cycle per minute for this example and was about 0.6 cycle per minute for one other run recorded.

[4]In figure 19, the indicated position of the recordings with respect to circumferential location is not significant. The leaders are used only to indicate axial position.

Selection of data. - In downflow the circumferential wall temperature variations were much more severe than they were in upflow. For low heating rates the averaging of data for pairs of thermocouples at each axial position resulted in a smooth average wall temperature curve, as indicated by figure 18(a). In that figure, symbols of the same kind are all on the same side of the tube and a smooth curve could be drawn through each set of symbols. The temperature differences across the tube are as high as 4° F for this particular run.

A different wall temperature behavior was observed at higher heating rates, as shown in figure 18(b). The points can be averaged to give a smooth curve up to a certain position, but then very large circumferential wall temperature differences exist for the rest of the tube, the differences being as high as 9° F. These temperatures are steady in time. The temperature pattern would indicate a cell flow. With a still further increase in power, the periodic fluctuations discussed previously appeared.

Since the flow is now down instead of up, the exit of the tube becomes the entrance. The asymmetries present in upflow do not exist at the top of the tube, nor was a dip in wall temperature ever observed there.

Only wall temperatures which fit the smooth curve before the sudden change in wall temperature distribution were used in plotting results to be compared with the analysis. All data are presented in tables V and VI of reference 5. The temperature of each individual wall thermocouple is reported in table VI of reference 5 along with the average wall temperature at each location.

CONCLUDING REMARKS

The fully developed solutions of the analysis are all in the nature of asymptotic solutions and are expected to apply only far from the entrance. The results of the experiment indicate that, for positive Rayleigh numbers, these solutions do apply, and the concept of locally fully developed results is established. It is also concluded that the boundary conditions associated with these solutions are physically realizable.

The results of the analysis were found to apply only for values of negative Rayleigh number which are small; for large negative Rayleigh numbers axial asymmetry and unsteady flow were observed, and these conditions make the analysis inapplicable.

The thermal entrance region analysis of Siegel, Sparrow, and Hallman for pure forced convection was experimentally confirmed. However, the

fully developed Nusselt number of 48/11, predicted for this situation, is difficult to verify experimentally because of the influence of free convection effects.

The transition observed during heating with upflow would lead to the conclusion that similar phenomena are likely to be encountered in other similar types of flows. This would be expected to occur, for example, in upflow of a heat-generating fluid in an insulated pipe. It is recommended that further experiments be run to establish the region of applicability of those portions of the analysis made in the Hallman thesis which were not investigated by the present experiment.

Lewis Research Center
National Aeronautics and Space Administration
Cleveland, Ohio, August 24, 1961

E-1407

APPENDIX A

SYMBOLS

A	axial temperature gradient in fluid, $\partial t/\partial x$, $^{\circ}F/ft$
c_p	specific heat of fluid at constant pressure, Btu/(lb)($^{\circ}F$)
D	tube inside diameter, ft
g	acceleration due to gravity, ft/sec^2
h	heat-transfer coefficient, q/θ_m, Btu/(sec)(sq ft)($^{\circ}F$)
I	test-section current, amp
k	thermal conductivity of fluid, Btu/(sec)(sq ft)($^{\circ}F/ft$)
k_f	thermal conductivity evaluated at film temperature
L	length of heated section, ft
Nu	Nusselt number, hD/k, dimensionless
Pr	Prandtl number, $\mu g c_p/k$, dimensionless
q	wall heat-flux density, Btu/(sec)(sq ft)
q_e	net electrical input to fluid, Btu/hr
q_{th}	thermal energy rise of fluid in passing through heated test section, Btu/hr
R	test-section resistance, ohms
Ra	Rayleigh number, $\rho^2\beta g^2 c_p D^4 A/16\mu k$, dimensionless
Ra_D	Rayleigh number based on diameter of tube, $\rho^2\beta g^2 c_p D^3(t_w - t_m)/\mu k$, dimensionless
Re	Reynolds number, $u_m D/\nu$, dimensionless
t	static fluid temperature, $^{\circ}F$
t_a	ambient temperature, $^{\circ}F$
t_e	exit temperature, $^{\circ}F$

t_m mixed-mean or bulk fluid temperature, °F

t_w inside tube wall temperature, °F

u_m mean velocity of fluid in tube, ft/sec

x distance measured along axis of tube upward from start of heated length, ft

β thermal coefficient of volume expansivity, $-\frac{1}{\rho}\left(\frac{\partial \rho}{\partial t}\right)_p$, (cu ft/°F)/cu ft

ϑ_m mixed-mean to wall temperature difference, °F

μ dynamic viscosity of fluid, (lb)(sec)/sq ft

ν kinematic viscosity of fluid, sq ft/sec

ρ mass density of fluid, $(lb)(sec^2)/ft^4$

Subscripts:

f film temperature

fd fully developed

APPENDIX B

ACCURACY OF RESULTS

Error Analysis

A detailed error analysis was made for one set of thermocouples in one run (run (U30)), and the result for Nusselt number was 6.12±0.25, or an accuracy of about 4 percent. The most important factor affecting the accuracy in this case was the accuracy of the temperature difference $t_w - t_m$. The uncertainty calculated here was the uncertainty based on 20 to 1 odds.

Factors Affecting Accuracy of Results

A heat balance between electrical energy input and the thermal energy increase of the fluid will give some indication of the magnitude of errors (known and unknown) which affect reduced quantities such as local mixed-mean temperature and wall heat flux. A plot of net electrical energy input (after heat loss corrections) against measured thermal energy rise is given in figure 20. A deviation from the line indicates an imperfect heat balance. Except for the two lowest power runs, the heat balance is within 6 percent, and for most runs it is much better. The heat balance improves with increase in power and in almost all cases the electrical input (after loss corrections) is greater than the thermal energy rise. Since, by the use of the a-c potentiometer, the electrical power measurement accuracy should be nearly independent of power level, it is felt that this discrepancy is largely due to errors in bus bar heat loss corrections and to errors in measuring bulk temperature rise. One would expect the percentage error in measuring a temperature difference with a calibrated thermocouple to become less as the temperature difference is increased. This is consistent with the trend in the heat balance data. It is concluded that the unknown error in overall heat balance is small.

There is some evidence that there are unknown errors in the measurement of wall temperature. These are felt to be largely caused by the influence of stray alternating current on the d-c thermocouple circuitry. The thermocouples were spot-welded directly to the test section, which was a-c resistance heated. An electronic null indicator was used with a Rubicon, Model B, potentiometer to measure thermocouple voltages. It was first observed that the null indicator lost sensitivity whenever a test-section thermocouple was being read. When connected to an oscilloscope, a 60-cycle a-c signal was observed. This could be eliminated by using a 400-microfarad capacitor across the input terminals to the potentiometer and by grounding one end of the test section (which previously had been floating). These changes gave good sensitivity except when

reading thermocouples near the ungrounded end of the test section. This problem was corrected by using a ground at each end and a toggle switch to select the end to be grounded. The sensitivity was good at each end and tolerable at the center of the test section. The central test-section thermocouple was read twice, once with each end grounded. The maximum discrepancy noted was 0.017 millivolt (about 0.5° F), and in most cases it was less than this.

The foregoing changes are believed to have removed the greatest part of this error but probably not all of it. One anomaly was that the standardization point of the potentiometer kept changing when a temperature traverse of the test section was being made. Apparently the alternating current still getting into the potentiometer affected the standardization point. The potentiometer was standardized before each thermocouple reading.

REFERENCES

1. Hallman, T. M.: Combined Forced and Free-Laminar Heat Transfer in Vertical Tubes with Uniform Internal Heat Generation. Trans. ASME, vol. 78, no. 8, Nov. 1956, pp. 1831-1841.

2. Gross, J. F.: Heat Transfer in Laminar Flow. Ph.D. Thesis, Purdue Univ., June 1956.

3. Donner, Thomas: Laminar Flow Heat Transfer in a Round Tube. M.S. Thesis, Rensselaer Polytech. Instit., Nov. 1957.

4. Ostroumov, G. A.: Free Convection Under the Conditions of the Internal Problem. NACA TM 1407, 1958.

5. Hallman, T. M.: Combined Forced and Free Convection in a Vertical Tube. Ph.D. Thesis, Purdue Univ., May 1958.

6. Hanratty, Thomas J., Rosen, Edward M., and Kabel, Robert L.: Effect of Heat Transfer on Flow Field at Low Reynolds Numbers in Vertical Tubes. Ind. and Eng. Chem., vol. 50, no. 5, May 1958, pp. 815-820.

7. Brown, W. G., and Grassmann, P.: Der einfluss des auftriebs auf wärmeübergang und druckgefälle bei erzwungener strömung in lotrechten rohren. Forsch. Geb. Ing.-Wes., Bd. 25, no. 3, 1959, pp. 69-75.

8. Tao, L. N.: On Some Laminar Forced-Convection Problems. Paper 60-WA-188, ASME, 1960.

9. Siegel, R., Sparrow, E. M., and Hallman, T. M.: Steady Laminar Heat Transfer in a Circular Tube with Prescribed Wall Heat Flux. Appl. Sci. Res., sec. A, vol. 7, no. 5, 1958, pp. 386-392.

10. Clark, J. A., and Rohsenow, W. M.: Local Boiling Heat Transfer to Water at Low Reynolds Numbers and High Pressure. Tech. Rep. no. 4, Div. Industrial Cooperation, M.I.T., July 1, 1952.

11. Scheele, George F., Rosen, Edward M., and Hanratty, Thomas J.: Effect of Natural Convection on Transition to Turbulence in Vertical Pipes. The Canadian Jour. Chem. Eng., vol. 38, no. 3, June 1960, pp. 67-73.

12. Eckert, E. R. G., Diaguila, Anthony J., and Livingood, John N. B.: Free-Convection Effects on Heat Transfer for Turbulent Flow Through a Vertical Tube. NACA TN 3584, 1955.

13. Kays, W. M.: Numerical Solutions for Laminar-Flow Heat Transfer in Circular Tubes. Trans. ASME, vol. 77, no. 8, Nov. 1955, pp. 1265-1274.

14. Marshall, Roland B.: Measurements in Electrical Engineering, pt. II. Second ed., John S. Swift Co., Inc., 1949.

15. Knudsen, James J., and Katz, Donald L.: Fluid Dynamics and Heat Transfer. McGraw-Hill Book Co., Inc., 1958, p. 228.

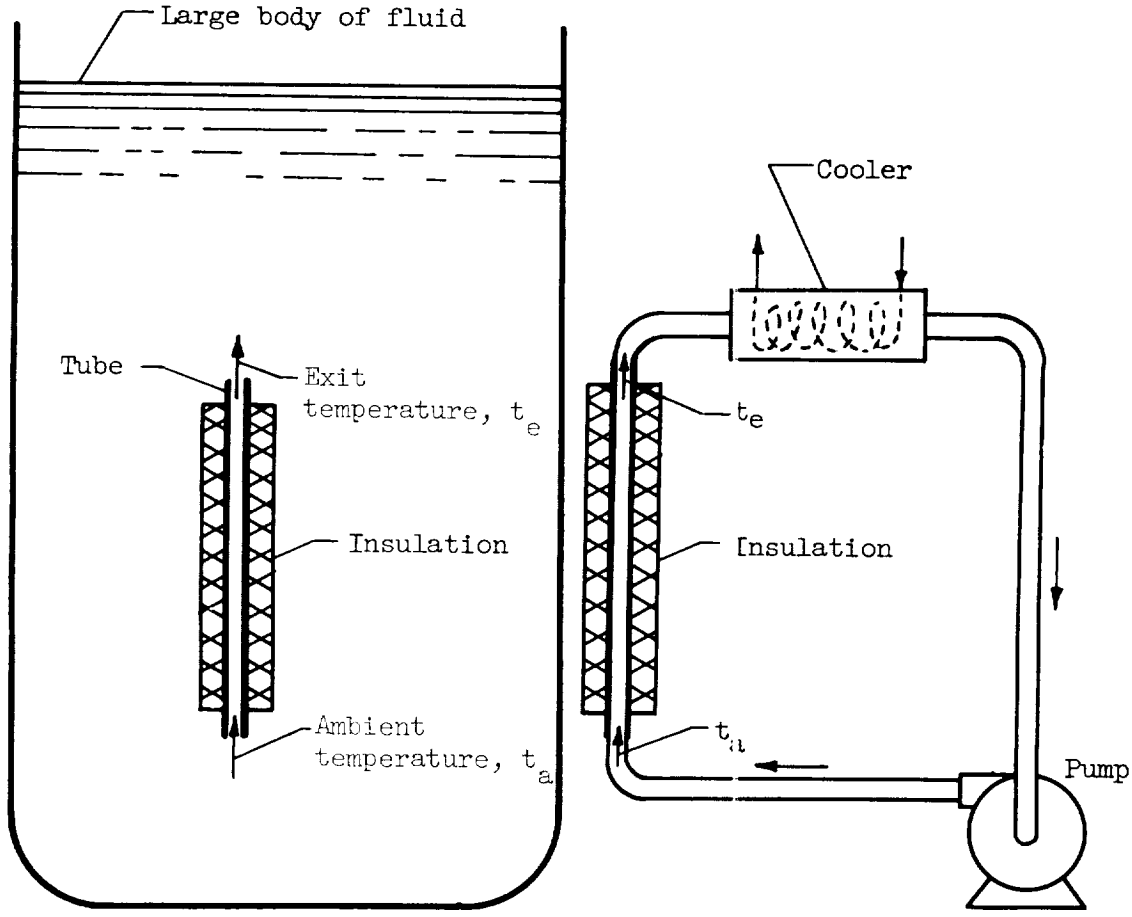

(a) Free convection.

(b) Combined forced and free convection.

Figure 1. - Combined forced and free convection.

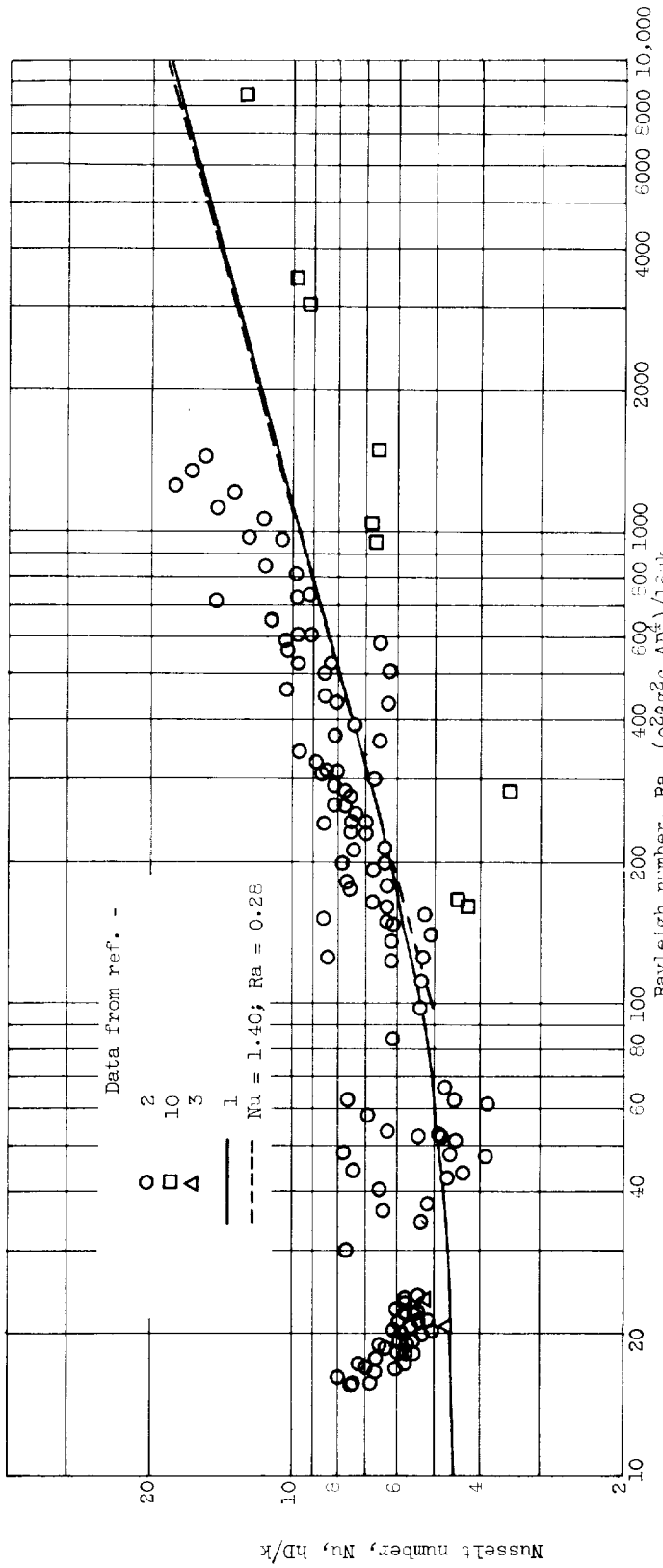

Figure 2. - Comparison between analysis of reference 1 and experiments of references 2, 3, and 10 for combined forced and free convection.

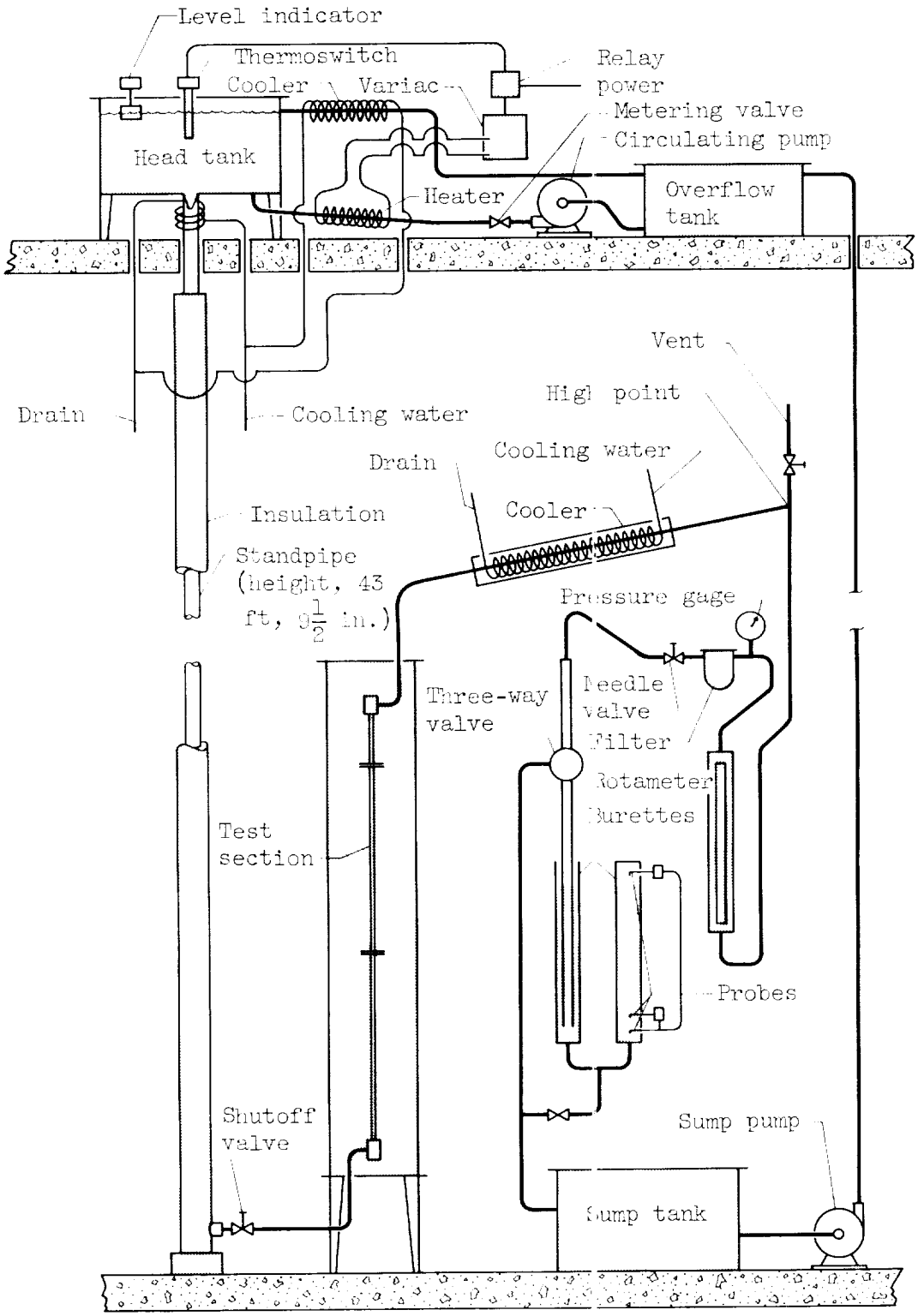

Figure 3. - Heat-transfer loop.

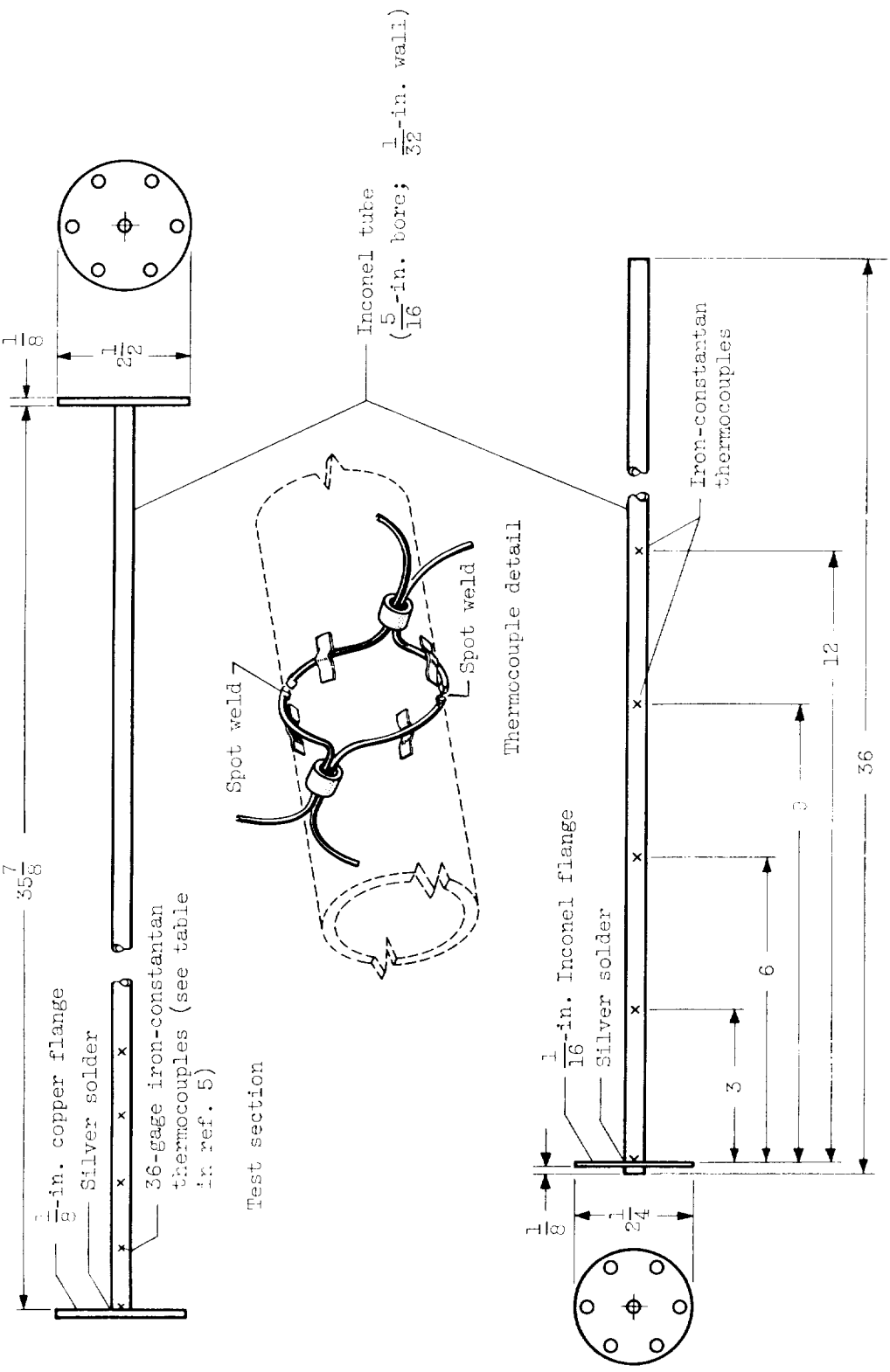

Figure 4. - Test section and approach section. (Dimensions are in inches.)

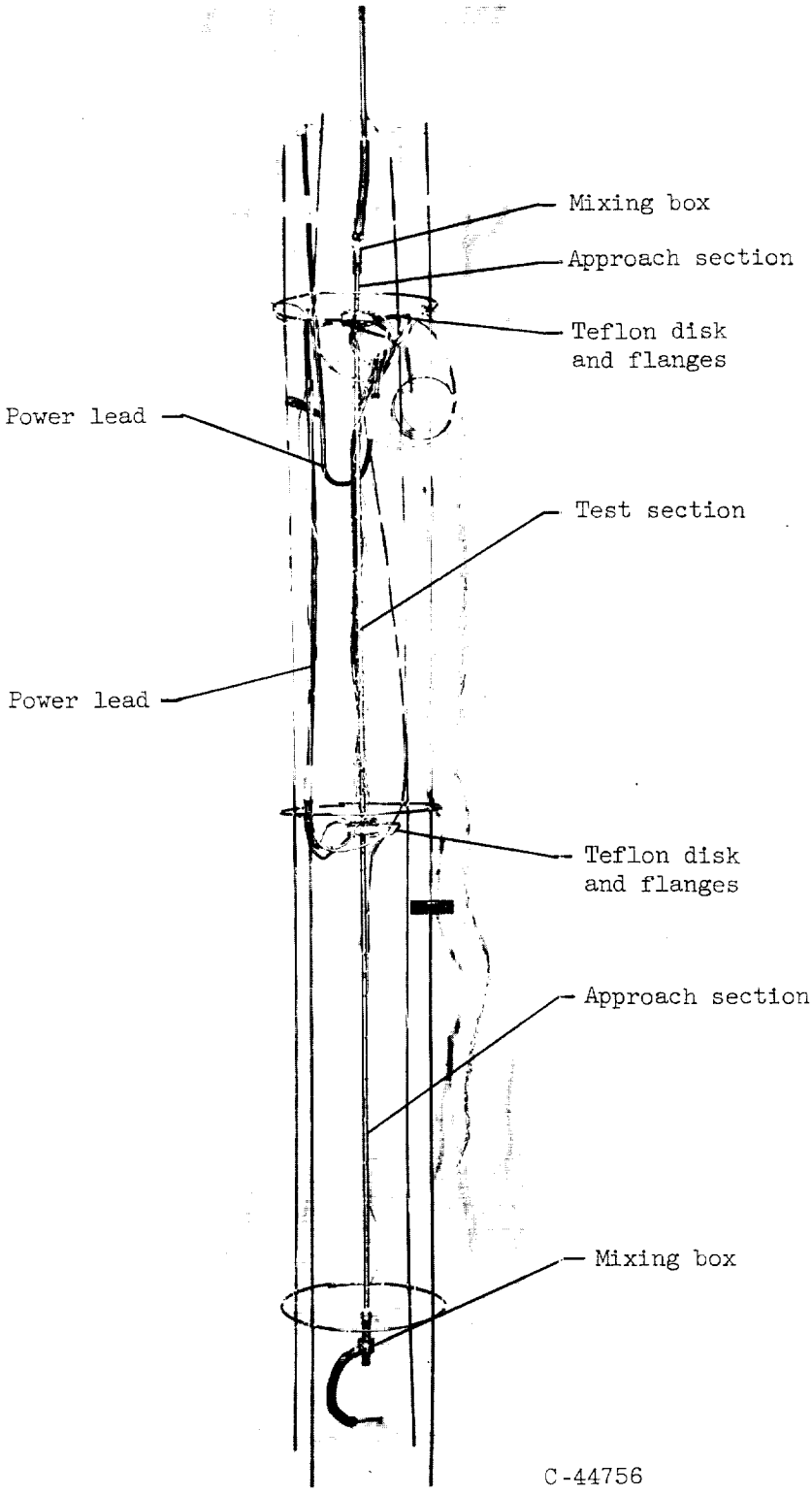

Figure 5. - Assembly photograph of test and approach sections (radiation shields removed).

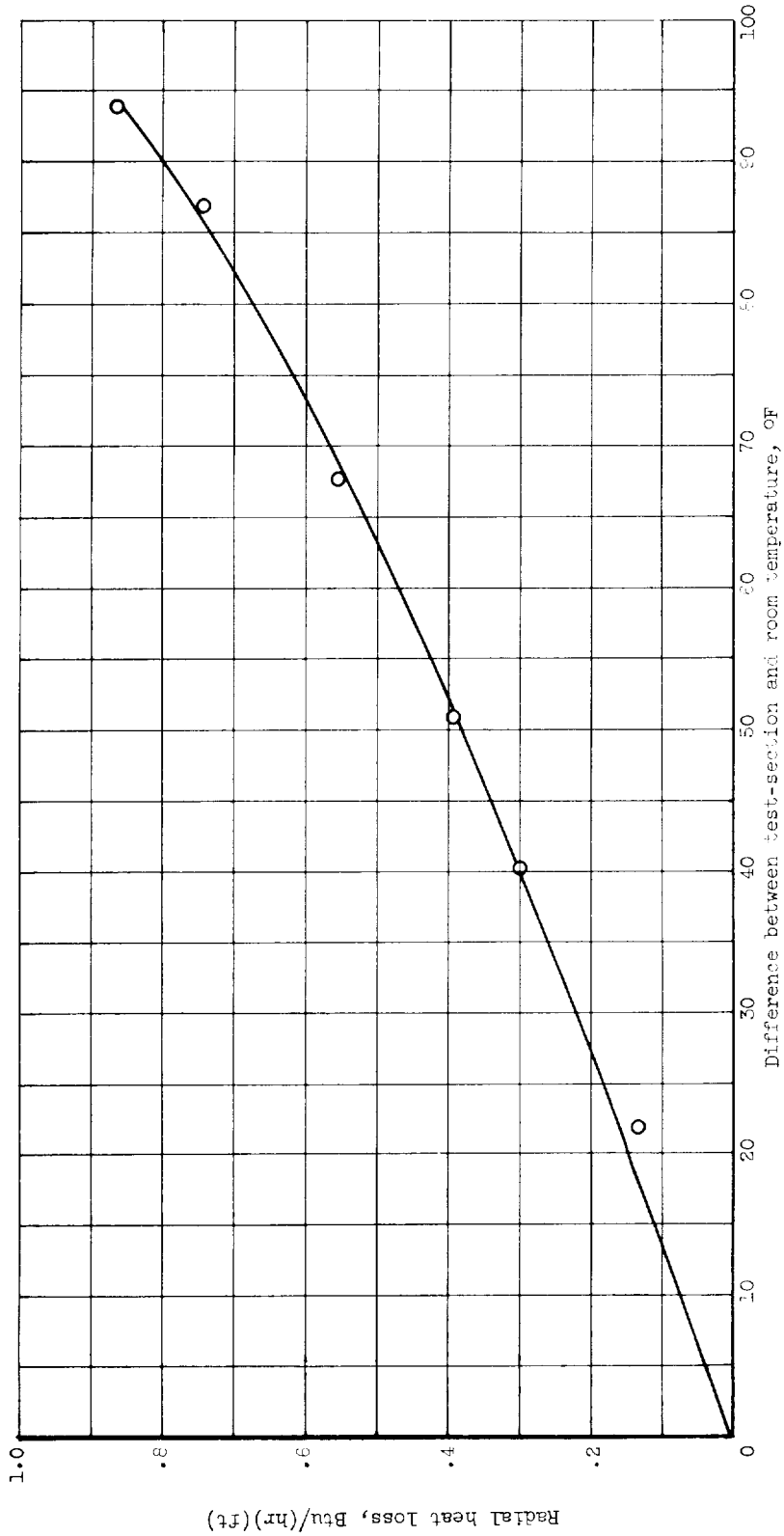

Figure 6. - Radial heat loss from test section.

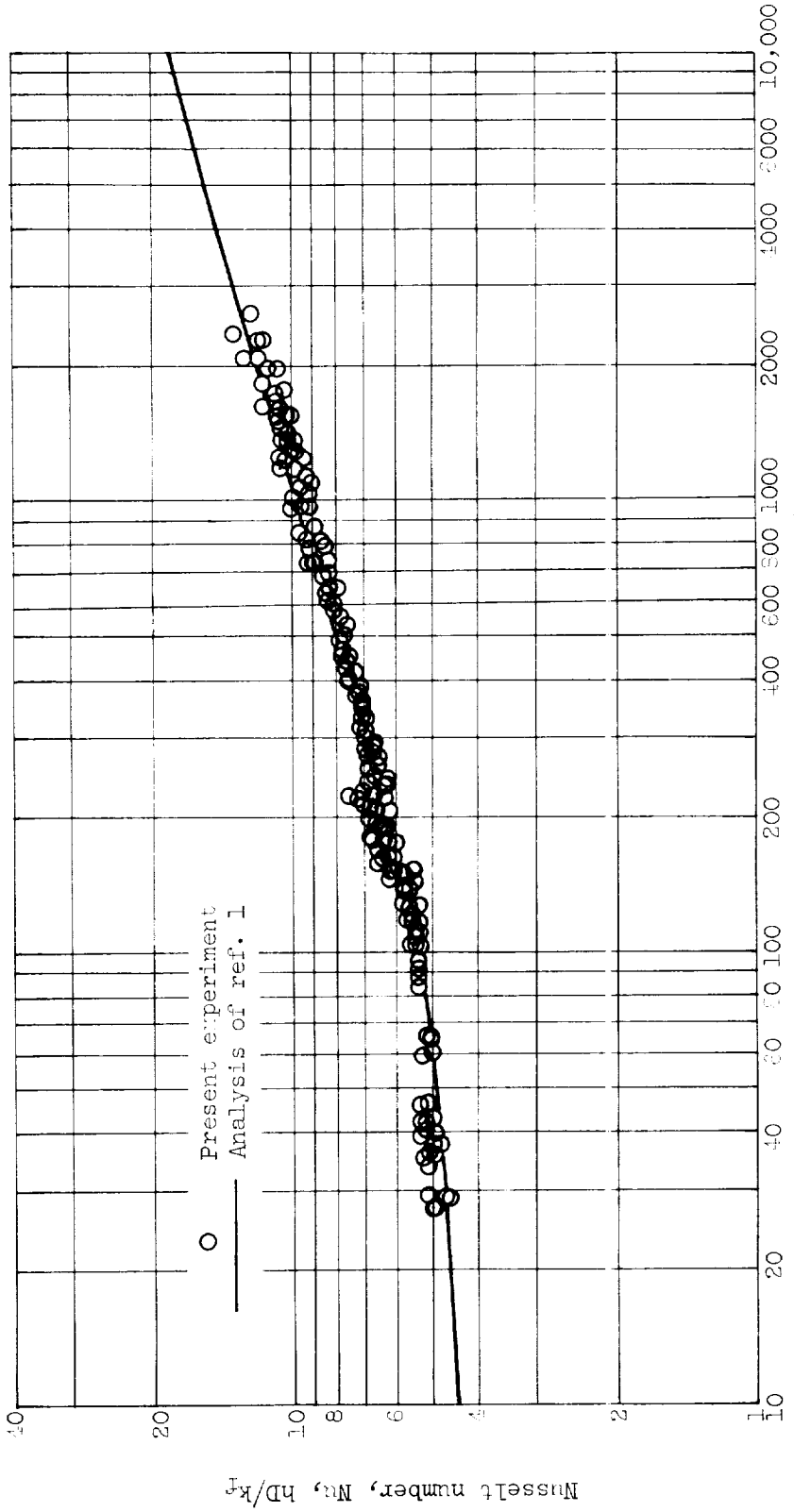

Figure 5. - Comparison of fully developed Nusselt numbers with analysis of reference 1 for upflow with heating.

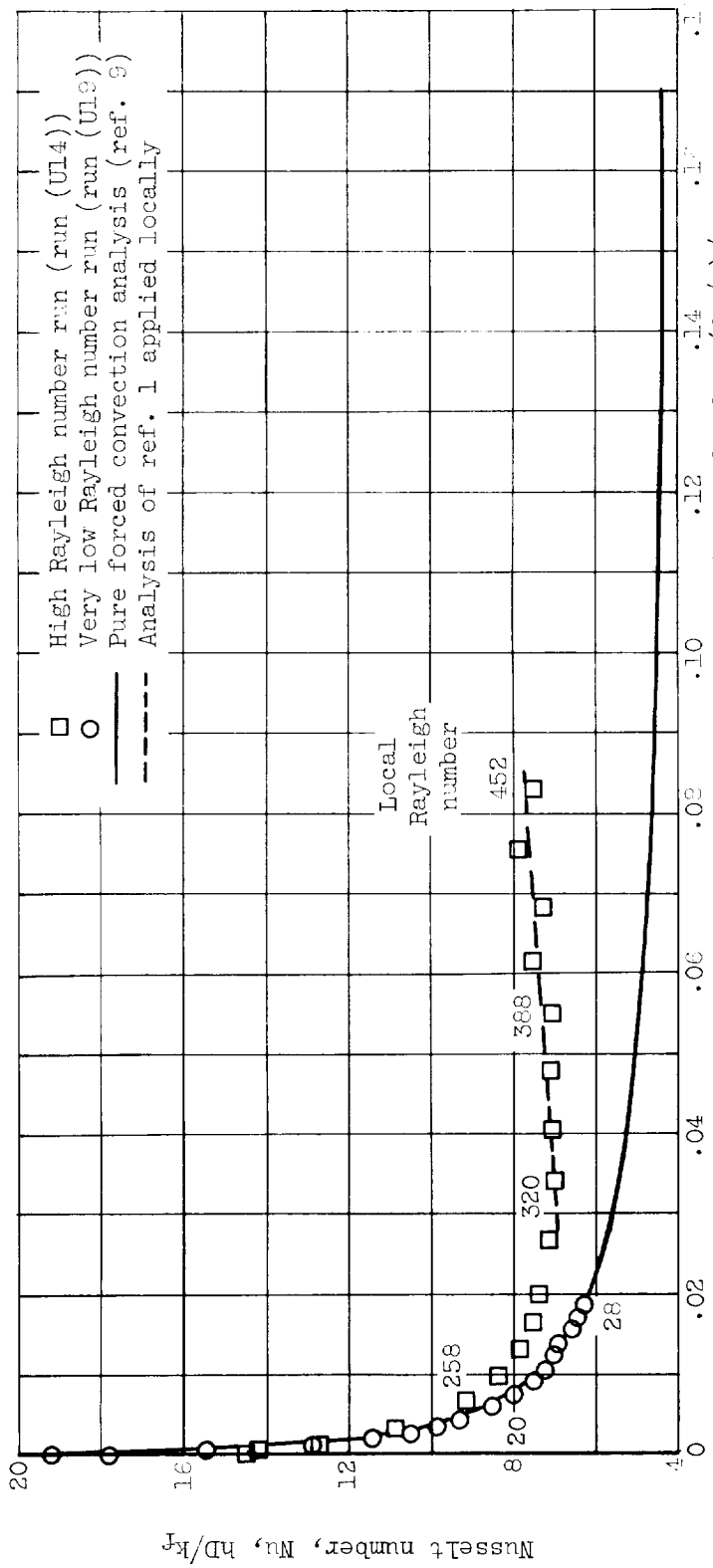

Figure 10. - Effect of Rayleigh number on entrance Nusselt number for upflow with heating.

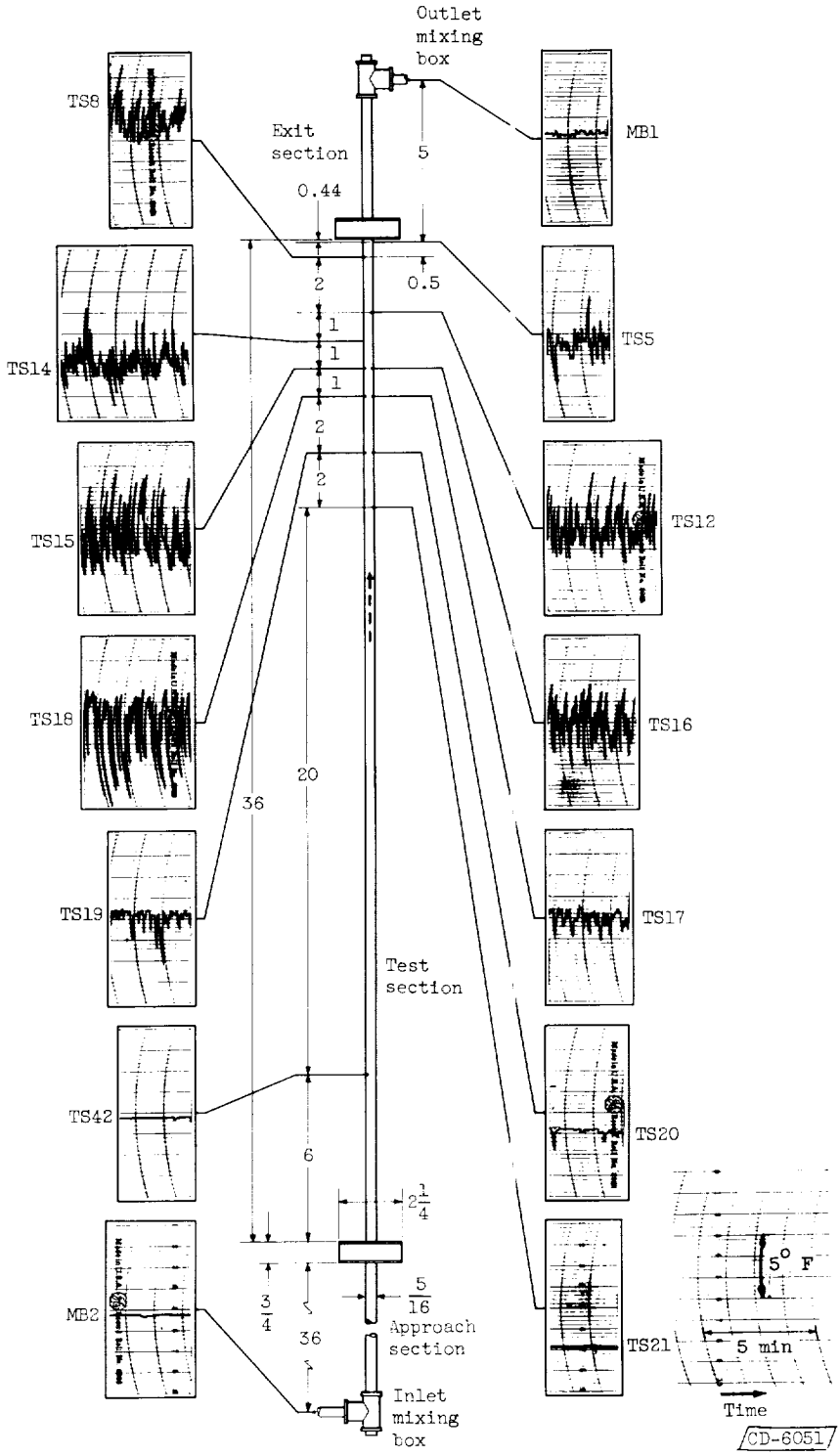

Figure 13. - Transient record of turbulent transition with heating during upflow. Run (U24); Rayleigh number, 1100; Reynolds number, 850. (Dimensions are in inches; TS and MB numbers identify test-section and mixing-box thermocouples, respectively.)

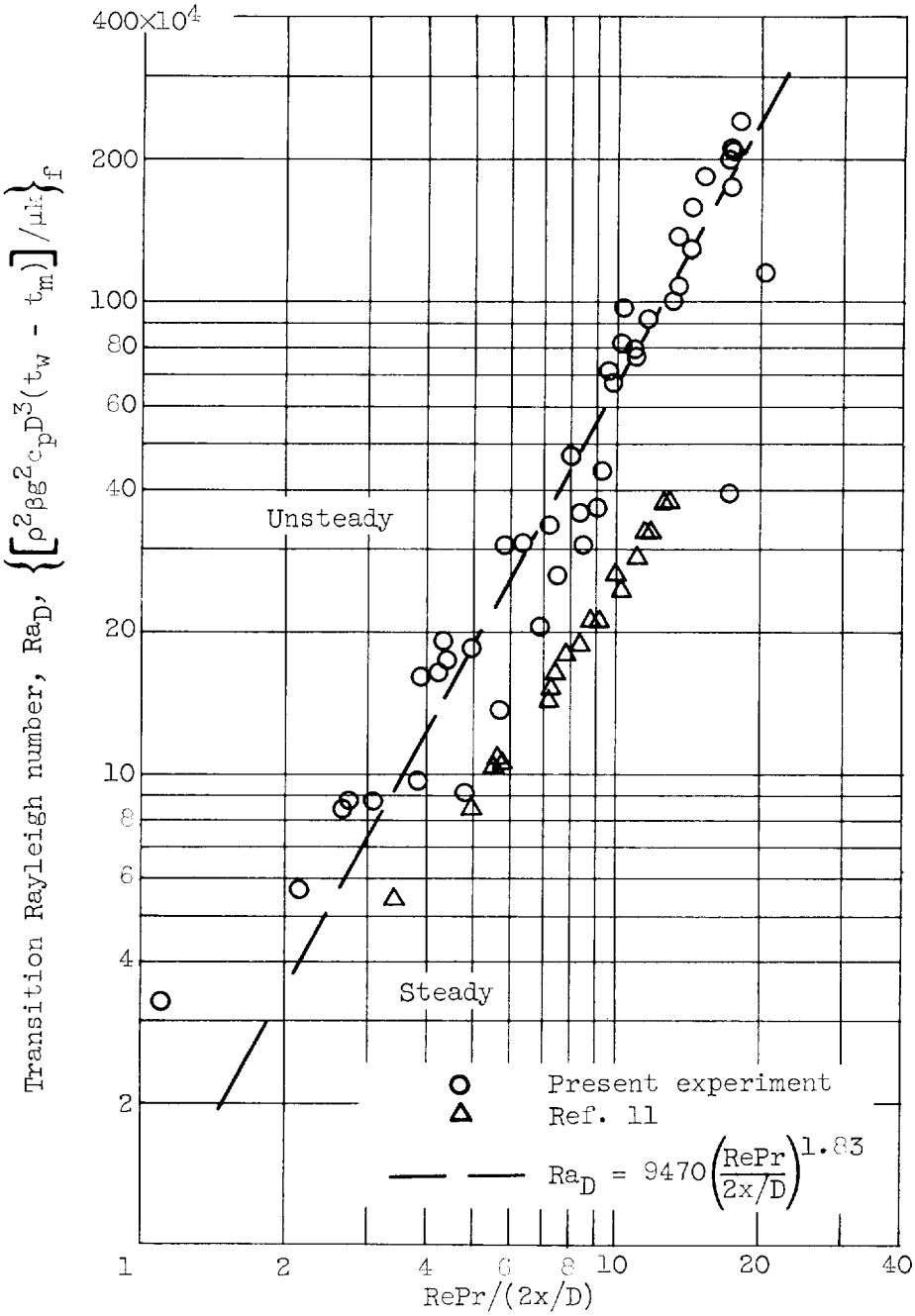

Figure 14. - Correlation of data for transition in upflow with heating.

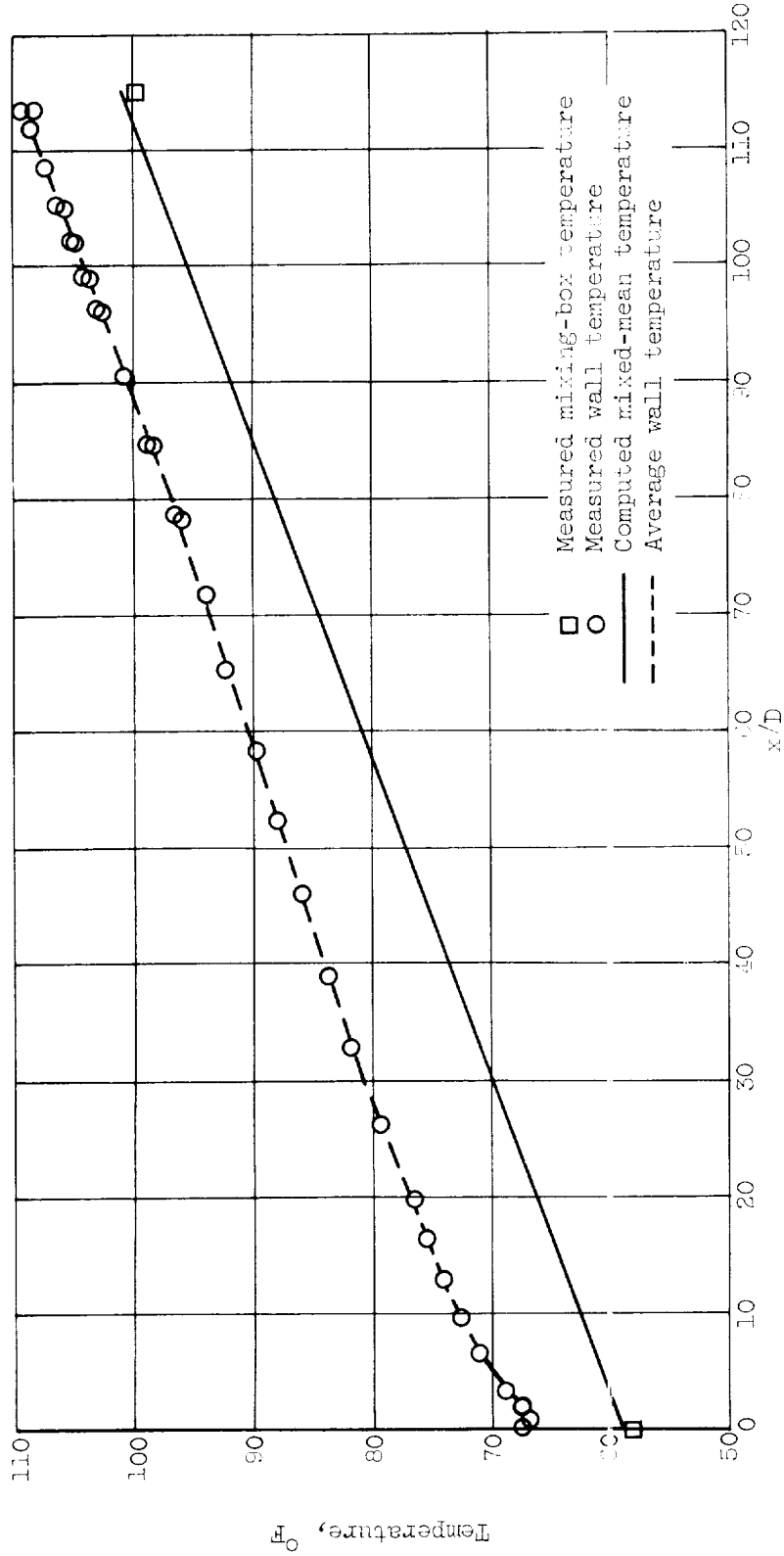

(a) Peclet number, 480 (run (U21)). Power, 57 watts.

Figure 15. - Representative wall temperature profile for upflow with heating.

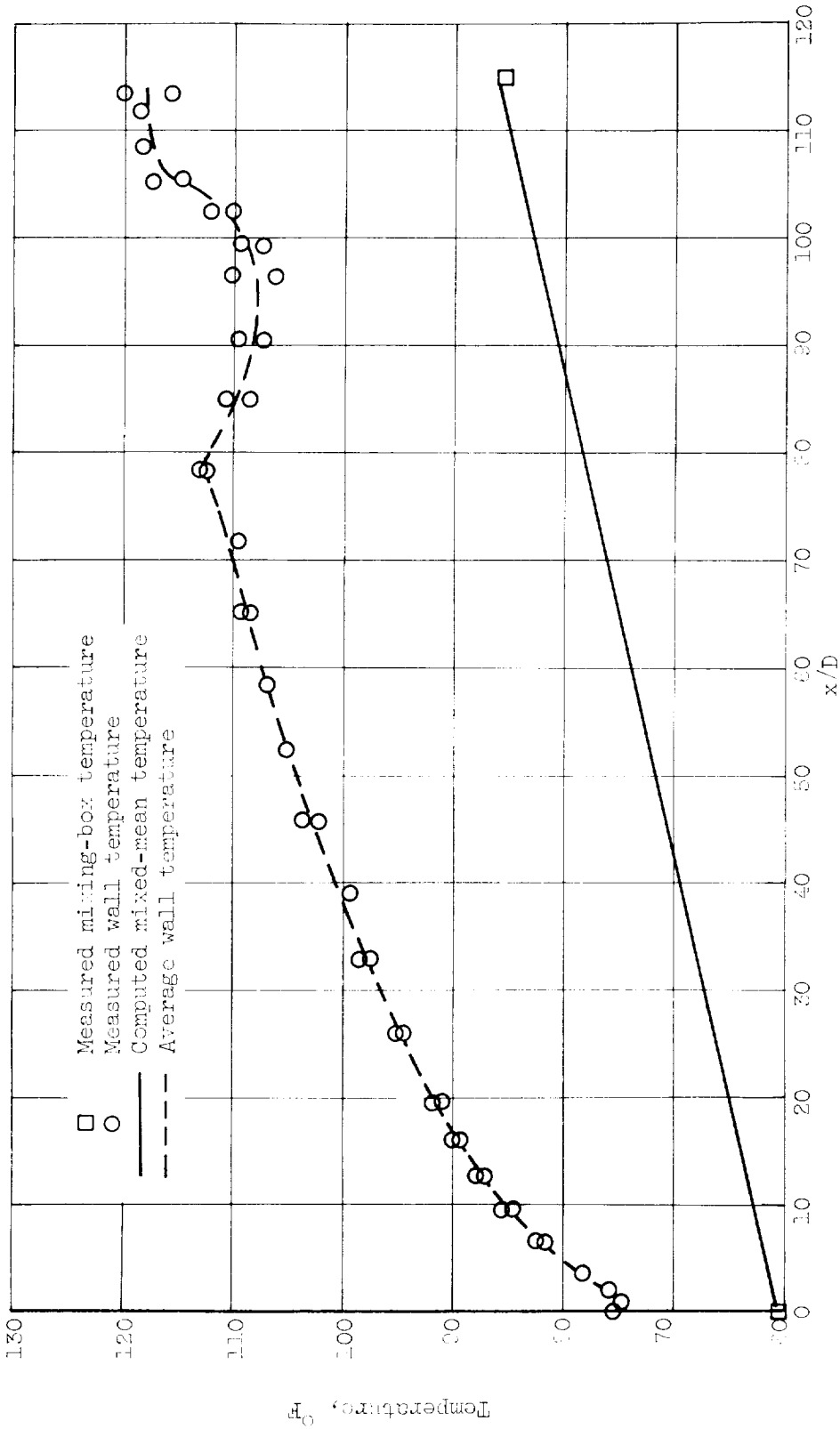

(e) Peclet number, 3.00 (rpm (UL)). Power, 1[illegible] watts.

Figure 15. - Concluded. Representative wall temperature profile for upflow with heating.

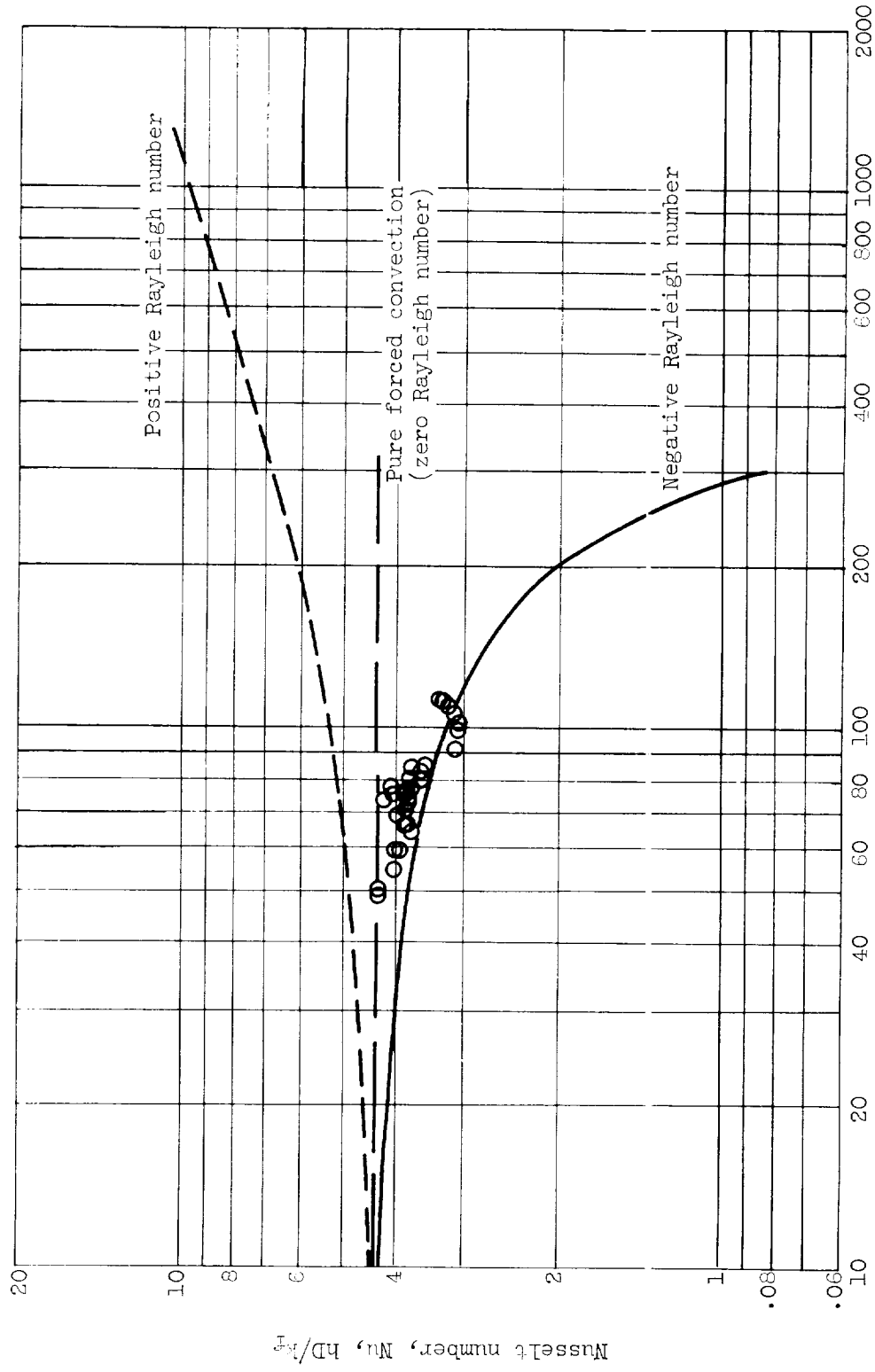

Figure 16. - Comparison of fully developed Nusselt numbers with analysis for downflow with heating.

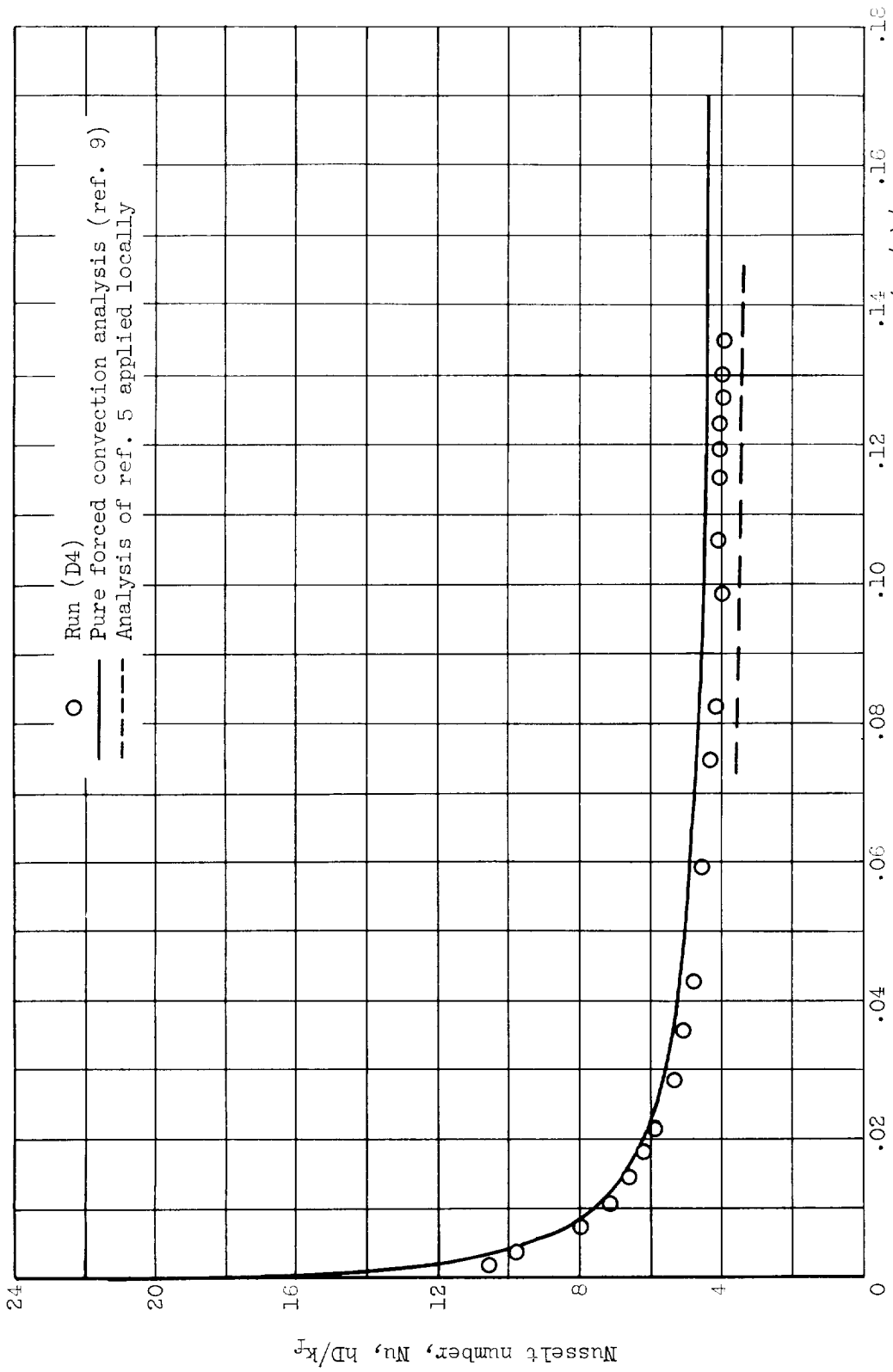

Figure 17. - Thermal entrance Nusselt number for negative Rayleigh number for downflow with heating.

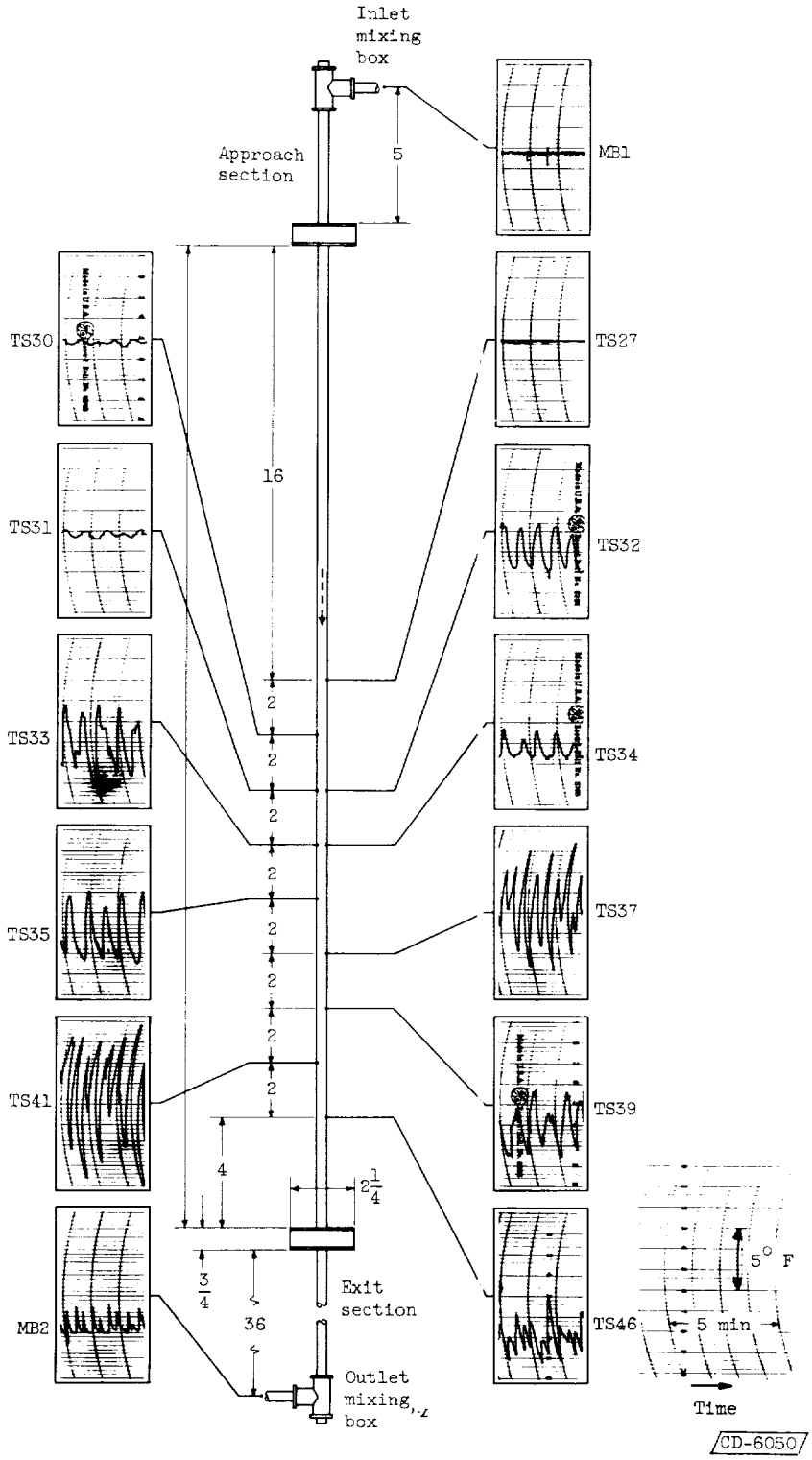

Figure 19. - Periodic wall temperature variations encountered with heating during downflow. Run (D12); Rayleigh number, -105; Reynolds number, 435. (Dimensions are in inches; TS and MB numbers identify test-section and mixing-box thermocouples, respectively.)

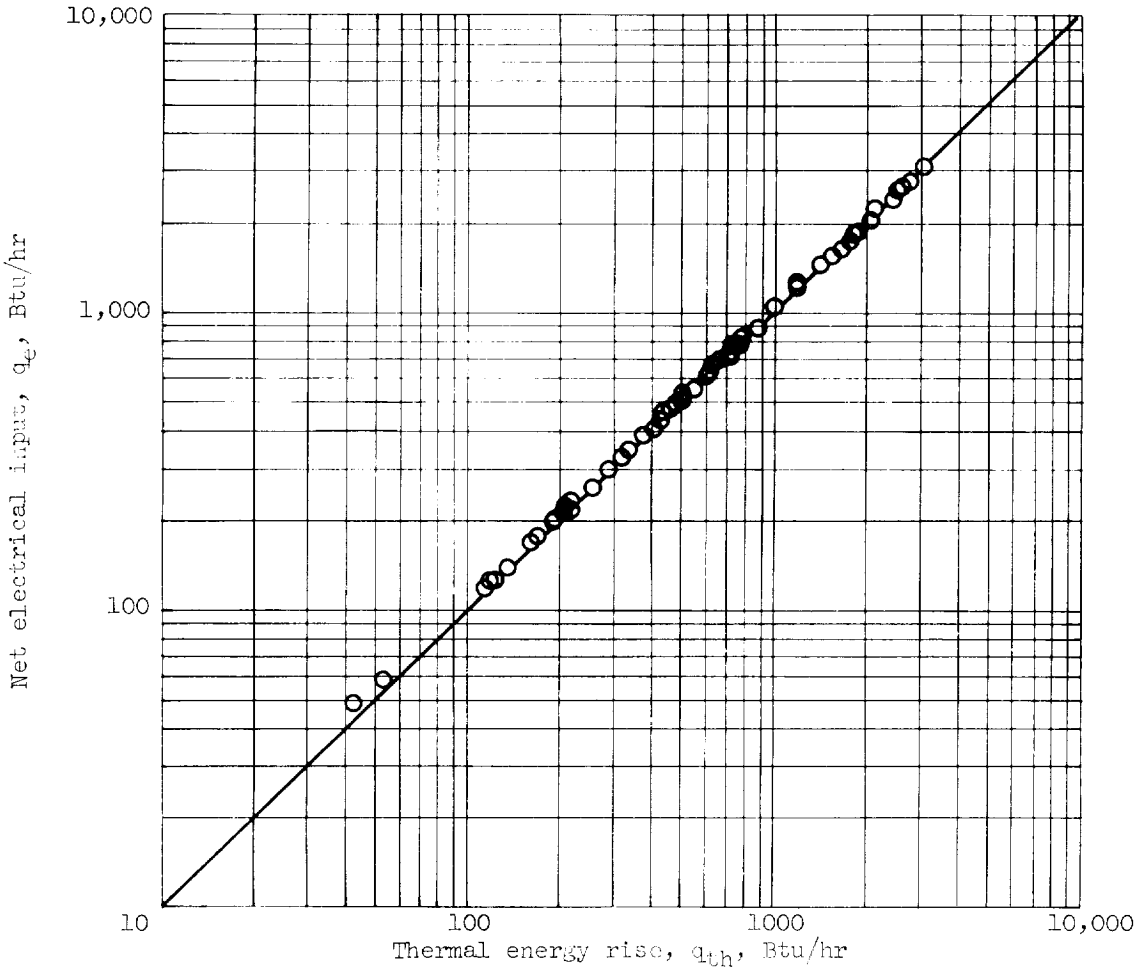

Figure 20. - Heat balance.

NASA-Langley, 1961 E-1407